Romanian Reports in Physics, Vol. 68, No. 4, P. 1506–1512, 2016

CEMS MEASUREMENTS ON LOW ^{57}Fe DOPED ANATASE NANOPARTICLES

I. BIBICU*, S. CONSTANTINESCU, D. TARABASANU-MIHAILA, M.N. GRECU

National Institute of Materials Physics, P.O.Box MG-7, RO-077125 Bucharest – Magurele, Romania,
*E-mail: bibicu@infim.ro

Received May 22, 2016

Abstract. We report the conversion electron Mössbauer spectroscopy (CEMS) used to analyze the iron valence states and magnetic ordering properties in ^{57}Fe low doped (0.1–1% at.) as prepared and annealed anatase TiO_2 nanoparticles. The spectra evidence the static and dynamic diversity of local defects around the Fe ions, localized mainly on the surface samples.

Key words: TiO_2, Fe-57, CEMS.

1. INTRODUCTION

Since several years there have been strong efforts to produce a new class of semiconductors: diluted magnetic semiconductor oxides (DMSO), for spintronics applications [1–5 and references therein]. These materials should expand the functionality of the common semiconductors by using not only the electrical charge but also the spin of the electrons for the information transfer. Recently, in Co-doped TiO_2 anatase thin film has been reported a ferromagnetic ordering even above 400 K with a magnetic moment of 0.32 μ_B per Co atom [4]. These results have motivated intensive experimental studies using different spectroscopic techniques. Titanium dioxide, one of the most studied oxide semiconductors due to its efficient photocatalytic activity [3], has raised the interest in its study as being potentially usable in spintronics applications as diluted magnetic semiconductor. On the other hand a great scientific interest concerns the mechanisms of observed magnetic ordering and charge transfer between the doping ions and constituents of hosting lattice [3–5]. A powerful tool to investigate nondestructively the magnetism of solids and the ionic states of its constituents is Mössbauer spectroscopy, which probes the Zeeman splitting and the valence of relevant nuclei and their ionic-hosts respectively. Moreover, the films and nanoparticles surfaces of DMSO could be investigated by conversion electron Mössbauer spectroscopy (CEMS). We note that CEMS methodology is rarely used due to its technical difficulties and relative complexity. In the last years, however, there are some

controversial discussions as regards the nature of ferromagnetism in Fe doped TiO_2 films investigated by CEMS [6–9].

In this report we are focus on CEMS surface analyze at room temperature on a series of as prepared and annealed ^{57}Fe doped TiO_2 nanoparticles with anatase structure. We have tried to find the ionic states of iron and their role in the enhancement of magnetic ordering.

2. EXPERIMENTAL

^{57}Fe-doped nanocrystalline titania powder were synthesised by a hydrothermal route at 200°C in a Teflon autoclave, starting with $TiCl_4$ and $^{57}FeCl_3.6H_2O$ (95.44% iron-57 isotopic enrichment) as precursors, and NH_4OH as precipitating agent [10]. Doped TiO_2 samples, with nominal concentrations of 0.1% at, 0.5% at and 1% at ^{57}Fe were synthesized. The annealing of samples was done in reduced air atmosphere at 650^o C for 2 hours, in a closed quartz tube.

The CEMS investigated samples obtained from as-prepared and annealed ^{57}Fe nanopowders, which have stirred with a solution of 5% collodion in amyl acetate. The obtained liquid suspension was further deposited like a "slurry" on a special flat horizontal measurement support. The liquid suspension has dried at room temperature. Then dried support introduced in the counter body and the as-prepared "film" has measured. Such preparation assures a preferential sedimentation function of nanoparticles dimension. The low dimension nanoparticles are presently, mainly in the upper part of the film. In a conventional transmission spectroscopy, the information is given by all nanoparticles, but in our measurements we have been obtained preferentially information from low dimension nanoparticles. Our test measurements showed that such samples preparation reduce the CEMS signal with around 40%. A maximum penetration depth of conversion electrons close to 125 nm (8–6 maximum monolayers of the mean crystalline size) is estimated in the thin solid film obtained after solution evaporation. CEMS spectra recorded in perpendicular backscattering geometry, *i.e.* with the incident γ-ray direction perpendicular to the sample plane, with a new homemade detector, gas-flow proportional detector with a 99% He + 1% C_4H_{10} mixture [11]. To obtain good CEMS spectra for low iron concentrations, a careful selection of window for single channel analyser done. The spectra have collected many hundreds hours in order to compensate the quite poor their statistics given by the complexity of spectra, iron low-concentration and of the expected intensity decreasing in the spectra, due to the sample preparation.

3. RESULTS AND DISCUSSION

XRD analysis has shown that all samples are a single phase with anatase structure. The lattice parameters determined by Rietveld structure refinements of

XRD patterns [12], are slightly increasing with Fe content. The mean crystallite sizes increase also from 16 nm to 24 nm in annealed samples.

The comparative Mössbauer spectra for the same doped sample with nominal concentrations of 0.1% at obtained by transmission spectroscopy and CEMS are given in Fig. 1. There is a significant difference between them and justify the reported research. The experimental and fitted CEMS spectra of samples are plotted in Fig. 2. The parameters, shown in Table 1, were calculated using a specialized fitting program, which assumes Lorentzian line resonances. The main constraints of the mathematical fit pattern consist in using the same full linewidths Γ and theoretical ratios between line resonances for hyperfine patterns. The spectra were fitted as overlapping of such patterns.

The spectra of as prepared samples show an intense quadrupolar contribution and overlapping magnetic patterns, revealing the presence of ^{57}Fe in nonmagnetic and magnetic ordering surroundings. The weight of the quadrupolar contribution tends to grow from 51% to 69%, with iron content. δ and Δ_Q of quadrupole doublet gently decreases to 0.31 mm/s and respectively increase from 0.19 mm/s to 0.58 mm/s with iron content. The line-width Γ has a decreasing tendency too. In the limits of errors, Fe^{3+} quadrupole pattern of 1% spectrum, (characteristic to isolated Fe^{3+} in TiO_2 lattice), has values closed to those report on 6% Fe: TiO_2 rutile films [6].

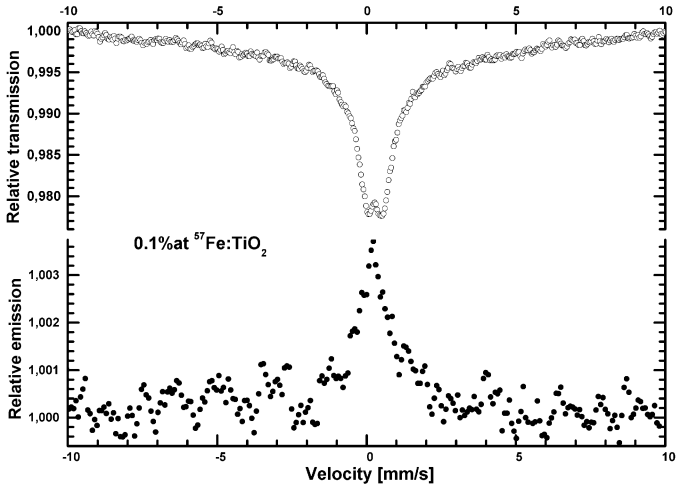

Fig. 1 – Comparative Mössbauer spectra for the same doped sample obtained by transmission spectroscopy and CEMS.

The magnetic contributions appear as "magnetic hyperfine fields distributions" (B_{hyp}), as taking into account the large Γ-values, $2\Gamma_s < \Gamma \leq 2.70$mm/s. The deconvolution shows more resolved B_{hyp} for 0.1% iron than for 1% sample.

Previous room temperatures CEMS measurements [7, 8] reveal B_{hyp} values of ~515 kGs and ~295 kGs, ~330 kGs, 483 kGs in spectra of iron doped rutile and anatase $TiO_{2-\delta}$ thin films, deposited on different substrates. The high values of B_{hyp} (~400 kGs, 382 kGs and 411 kGs) in our CEMS spectra are given in Table 1, for 0.1% and 0.5% samples. These are accompanied by medium B_{hyp} = (290–140) kGs and low B_{hyp} = (90–30) kGs values.

The ferric (0.10 mm/s < δ < 0.50 mm/s) and ferrous (0.60 mm/s < δ < < 0.90 mm/s) ions, with $B_{hyp} \geq 400$ kGs and respectively B_{hyp} = 382 kGs and lower one, are detected in 0.1% at and 0.5% at samples with decreasing areas (from ~20% to ~17% and from ~19% at to ~12% at for Fe^{3+} and respectively Fe^{2+}), and near symmetric surroundings ($\Delta_Q \leq 0.15$ mm/s). No magnetic characteristic sextets to metallic Fe agglomeration, or Fe_3O_4 magnetic ordered phases has been detected here. Two magnetic patterns observed in 0.5% spectrum could suggest Fe-O bonds in superficial sheets of our "film-like" TiO_2 nanoparticles. Fe-species with 0.00 mm/s < δ < 0.10 mm/s and B_{hyp} < 300 kGs are in agreement with the reported data of 6% Fe:TiO_2 film [6], suggesting the high-spin Fe^{4+} ions. The possible presence of Fe^{4+} ions in ^{57}Fe:TiO_2 is in according to Ref. 13. Ferric ion can act as both electron and hole traps, to enhance their lifetimes, on condition of Fe-surface localization. Inside of TiO_2 nanoparticles and films iron acts as recombination centre. So, the detected Fe^{4+} seems to be localized on surface of our anatase nanoparticles.

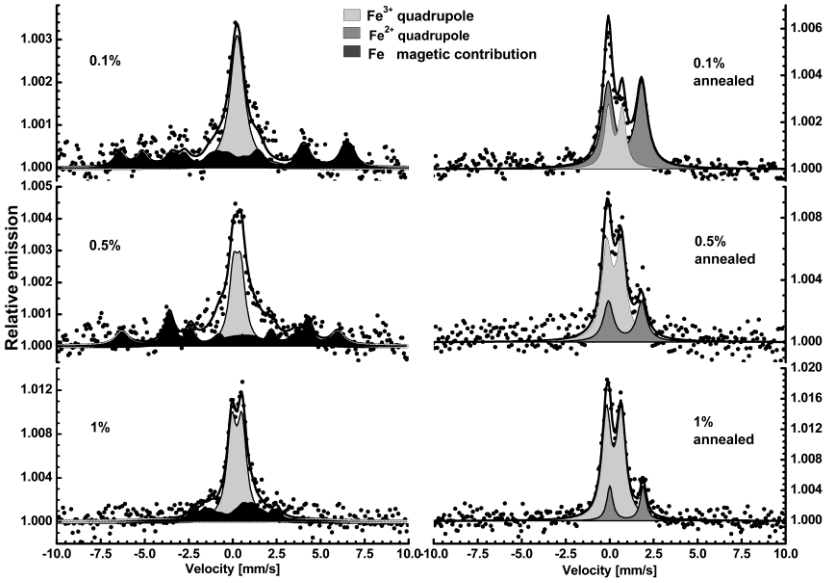

Fig. 2 – Magnetic and nonmagnetic contributions in CEMS spectra of ^{57}Fe:TiO_2 nanoparticles (● data; ▬ fit).

The mechanisms of magnetic ordering in transition metal doped TiO_2 is still an open problem, specially due to the evidence of room temperature ferromagnetism in undoped TiO_2 [14], attributed to defects and oxygen vacancies. Among the possible models proposed to explaine this, the bond magnetic polarons model has received the great attention [5, 12 and references therein]. The basic idea for $Fe:TiO_2$ system is the polarization of iron ion spins by defects enhances the magnetism already present.

The disappearance of the magnetic contribution in the system was observed by annealing procedure. The deconvolution of annealed samples spectra shown in Fig. 2 reveals a superposition of two doublets, corresponding to Fe^{3+} and Fe^{2+} ions, as well the lack of the initial magnetic contribution. No Fe^{4+} patterns have been detected. A redox reaction has occurred during the annealing treatment in a reduced air atmosphere at 650°C. The Fe^{3+}-quadrupole doublets are more intense as iron content increases. Their δ values, closed to those reported [6, 7] exhibit the iron substitution of Ti^{4+} in the lattice. Γ values of the two kind of doublet patterns are enough large to suggest a distribution of iron environments distinguishable by the different repartition of oxygen vacancies, and Ti and Fe ions in the second and third neighbourhood.

Table 1

The Mössbauer hyperfine parameters of the CEMS spectra in $^{57}Fe:TiO_2$

Sample	**δ* [mm/s]**	**Δ_Q/ε_Q** [mm/s]**	**B_{hyp} [kGs]**	**Γ*** [mm/s]**	***A*** **[%]**	**estimated Fe valence**
0.1 % at	0.23	–0.15**	411	0.80	19.7	3+
	0.88	0.04**	382	0.74	19.4	2+
	0.03	0.12**	89.8	0.77	9.7	4+
	0.38	0.19	–	0.95	51.2	3+
0.5 % at	0.10	–0.09**	400	0.89	17.3	3+
	0.01	0.23**	258	0.58	19.0	4+
	0.65	–0.10**	54	1.89	11.9	2+
	0.36	0.44	–	0.64	51.8	3+
1 % at	0.07	–0.03**	287	2.70	7.8	4+
	0.05	0.20**	147	0.54	12.4	4+
	0.51	–0.77**	34	0.74	14.2	3+
	0.31	0.58	–	0.62	65.6	3+
0.1 % at annealed	0.44	0.86	–	0.51	30.9	3+
	1.07	1.84		0.80	69.1	2+
0.5 % at annealed	0.36	0.85	–	0.71	69.8	3+
	1.02	1.84		0.70	30.2	2+
1 % at annealed	0.35	0.86	–	0,64	81.7	3+
	1.10	1.95	–	0.42	18.3	2+
Errors	±0.03	±0.05	±6	±0.05	±5	

*δ is isomer shift relative to α-Fe; **Δ_Q, ε_Q are quadrupole split /shift parameter; ***$\Gamma = \Gamma_s + \Gamma_{abs}$, $\Gamma_s = 0.11$ mm/s;

The Fe^{2+} – quadrupole doublets have approaching the same values of δ and Δ_Q, in the limits of errors, but the patterns are less intense *vs.* Fe content. One remarks the different Fe^{2+} quadrupole parameters relative to those of FeO (δ = 0.93 mm/s and Δ_Q = 0.8 mm/s) or $FeTiO_3$ (δ = 1.08 mm/s and Δ_Q = 0.66 mm/s) phases. Besides, the hyperfine parameters values are closed to those reported in [8], suggesting the detection of the ferrous ionic surrounding similar to Fe_2TiO_4 phase, activated by the annealing procedure. The turning of ratio Fe^{2+}, Fe^{3+} doublets areas A_{Fe2+}/A_{Fe3+} from 69.1/30.9 to 18.3/81.7 *vs.* iron content, show the limits of the oxidation process.

The increasing tendency of Δ_Q-values and its limit [6], observed in quadrupole patterns of spectra, suggest Ti^{4+} substitution by isolated high spin Fe^{3+} in octahedral sites of anatase lattice. Indeed, taking into account the ionic radii of high and low spin Fe^{3+} (about 0.079 nm and 0.069 nm) while the octahedral Ti^{4+} is 0.075 nm, the growing of lattice parameters of Fe in anatase TiO_2 [12], indicates an overweight of ferric ion substitution.

The main evidence in the annealed-sample spectra consists in the lack of the magnetic ordering. This suggests that partial oxidation/reduction processes are accompanied by the breaking up the magnetic ordering during the annealing treatment.

4. CONCLUSIONS

The evidence of the Fe^{2+}, Fe^{3+} and the suggested presence of Fe^{4+} are related to the surface oxygen vacancies around the magnetic ions. Ferric iron plays the role of a trap for different type of defects. It is known that defects induced by doping create charge imbalance of host lattice. The diversity of iron valence states, the presence of magnetic patterns with large line widths in as prepared samples, and the breaking up of magnetic ordering to a specific annealing treatment, evidence the dynamic diversity of the local defect configurations around ^{57}Fe, and the role of the magnetic ions in the enhancement of magnetic ordering in anatase TiO_2 structure.

Acknowledgements. We gratefully acknowledge financial suport from CNCSIS –UEFISCSU, Romanian project PNII–IDEI nr. 4/2010, cod ID-106 and Core Program (contract PN 09-45).

REFERENCES

1. T. Dietl, H. Ohno, M. Matsukara, J. Cibert and D. Fernand, Science **287**, 1019-1022 (2000).
2. M. Venketesan, C.B. Fitzgerald and J.M.D. Coey, Nature **430**, 630-630 (2004). doi:10.1088/0268-1242/20/4/012
3. A. Hagfeldt, M. Gratzel, Chem. Rev. **95**, 49-68 (1995).
4. T. Fukumura, H. Toyosaki and Y. Yamada, Semicond. Sci. Technol. **20**, S103-S111 (2005).

5. J.M.D. Coey, K. Wongsaprom, J. Alaria and M.Venkatesan, J. Appl. Phys. **41**, 134012 (2008).
6. K. Nomura, K. Inaba, S. Iio, T. Hitosugi, T. Hasegawa, Y. Hirose and Z. Homonnay, Hyperfine Interactions **168**, 1065-1071 (2006).
7. K. J. Kim and Y. R. Park, J. Korean Phys. Soc. **48**, 1422-1426 (2006).
8. K. Nomura, H. Eba, K. A. Rykov and T. Hasegawa, Thin Solid Films **515**, 8649-8652 (2007).
9. G. Talut, H. Reuther, J. Grenzerand, S. Zholu, Hyperfine Interactions **191**, 425-432 (2009).
10. L. Diamandescu, M. Feder, D. Tarabasanu-Mihaila, F. Vasiliu, Appl. Catalys. A **325**, 270 (2007).
11. I. Bibicu, G. Nicolescu and C.Cretu, Hyperfine Interactions **192**, 85-91 (2009).
12. M. N. Grecu, S. Constantinescu, D. Tarabasanu-Mihaila and I. Bibicu, Phys. Status Solidi B **248**, 2927-2931 (2011).
13. Z. Li, W. Shen, W. He and X. Zu, J. Hazard. Mater. **155**, 590-594 (2008).
14. N. H. Hong, J. Sakai, N. Poirot and V. Brizé, Phys. Rev. B **73**, *13*, 132404 (2006).